Composite Interfaces, Vol. 15, No. 2–3, pp. 111 – 129 (2008)

Also available online - www.brill.nl/ci

Polypropylene-natural fibre composites. Analysis of fibre structure modification during compounding and its influence on the final properties

DEBORA PUGLIA [1], ANDREA TERENZI [1], SILVIA E. BARBOSA [2] and JOSÉ M. KENNY [1,*]

[1] *Materials Engineer Center, University of Perugia, Località Pentima Bassa, 21 - 05100 Terni, Italy*
[2] *Planta Piloto de Ingeniería Química, PLAPIQUI (UNS-CONICET), Cno. La Carrindanga Km. 7 - 8000 Bahía Banca, Argentina*

Received 15 September 2006; accepted 22 February 2007

Abstract—The final properties of composite materials are highly dependent on the residual geometrical parameters (length, diameter, aspect ratio), orientation and distribution of the fibres in the matrix, which in turn are related to the processing conditions. This study analysed the fibre structure variation during the processing of a polypropylene matrix reinforced with cellulose flax pulp for different reinforcement concentrations. The fibre's geometrical parameters, length, diameter and aspect ratio have been measured and their statistical distributions have been assessed for each concentration. Furthermore, the effect of the microstructure variation on the final mechanical properties was analysed. In particular, changes in the interfacial area were evaluated based on the hypothesis that the fibres were cylindrical in shape and considering the average values of the diameters and the lengths calculated using a statistical distribution approach. The fibre interfacial area after the process decreases as the fibre concentration increases and this evaluation explains how the adhesion methods that are used for fibre surface modification fail because of the decrement in the modifier interfacial density. The Halpin–Tsai approach was used to model the experimental data obtained from tensile tests for different composites, so as to confirm the effect of fibre parameters, such as aspect ratio and interfacial area values, in the PP/cellulose blends final properties.

Keywords: Natural fibre composites; fibre damage; aspect ratio; interfacial area; cellulose polypropylene composites.

1. INTRODUCTION

During the past few decades, composite materials have increased their market and applications due to the possibility of obtaining a very wide spectrum of properties;

*To whom correspondence should be addressed. E-mail: jkenny@unipg.it

in fact, each fibre–matrix combination can give different characteristics. The fibres used are usually of glass, aramid or carbon. In particular, carbon and aramid fibres are usually used for high performance composites due to their properties and cost, while glass fibres are used for large volume production composites due to the good compromise between low cost and good performance. In particular, short glass fibre composites are widely used in many applications since they combine a low processing cycle time with good mechanical performance. However, traditional reinforcements have some disadvantages: the cost is generally high, the recycling possibilities are low and the environmental impact is high because they do not use natural and renewable resources. Moreover, glass fibres can cause skin irritation during processing and handling and give slag during the burning of the material at the end of its life time [1–5].

In the last few years, both academic and industrial researchers have been working in order to find a good replacement for traditional glass fibres, to overcome these drawbacks and to satisfy requirements such as low cost, low environmental impact, properties comparable to traditional reinforcements and availability. Cellulose fibres present many advantages in comparison to synthetic ones, which make them attractive as reinforcements in composite materials. They come from abundant and renewable resources at a low cost, which ensures a continuous fibre supply and a significant saving in the costs of materials for the plastics industry. Despite the low strength of cellulose fibres, they can lead to composites with high specific properties because of their low densities. Unlike brittle fibres, such as glass and carbon fibres, cellulose fibres are flexible and fracture less when processed over sharp bends. This enables the fibres to maintain the desired aspect ratio for good composite performance.

Their non-abrasive nature permits high volume fraction filling during processing, increasing the composite's mechanical properties without the usual problems of machine wear associated with synthetic fibres, especially glass and ceramic. Cellulose fibres are also non-toxic, easy to handle and present none of the health problems of glass fibres, which can cause skin irritations and respiratory diseases when the fibrous dust is inhaled. They have the capability of surface modification (due to the high hydroxyl content), have low cost, require low amounts of energy for processing and are biodegradable [6–11].

The natural fibre composites (mainly with thermoplastic matrices) are currently used in many industrial fields for non-structural applications. These materials are applied in civil construction industries for the production of tiles, doors, windows, etc. In the automotive sector, different interior parts and panels are currently produced in natural fibre composites using different vegetable reinforcements [12–14]. There are a wide variety of cellulose fibres that can be used to reinforce thermoplastics. These include wood fibres, such as steam-exploded fibres and a variety of agro-based fibres such as stems, stalks, bast, leaves and seed hairs.

Despite the advantages mentioned above, the use of cellulose fibres in thermoplastics has not been extensive. Possible reasons that contribute to the unsatisfac-

tory final properties of the composite include poor dispersion characteristics in the non-polar, olefinic thermoplastic melt due to strong hydrogen forces between the fibres [15] and limited compatibility with many thermoplastic matrices. As a consequence thereof, the composites produced have poor mechanical properties [16]. The incorporation of cellulose fibres in synthetic polymers is often associated with a lack of fibre dispersion due to the wide differences in polarity and also the strong intermolecular hydrogen bonding between the fibres. This lack of fibre dispersion can result in clumping and agglomeration of cellulose fibres [17], which act as stress concentration points, initiating cracks during loading. This problem can be overcome by pre-treating the fibres with polymer coating materials. Another approach involves the use of dispersion aids, such as stearic acid, which facilitates fibre dispersion by decreasing both the size and number of fibre aggregates. As a result, the fibre-to-fibre interaction is significantly reduced and fibre wetting on the polymer matrix is improved.

Generally, the short fibre reinforcement effect in a thermoplastic matrix is governed by the following parameters: (i) fibre dispersion, (ii) fibre–matrix adhesion, (iii) fibre aspect ratio, (iv) fibre orientation and (v) fibre concentration (volume fraction). Studies for understanding the influence of these factors on cellulose-based composites have been carried out and reported in the literature by many researchers [17–21].

Aspect ratio variation is an important parameter to be taken into account in the improvement of fibre–matrix adhesion. In this sense, good interfacial adhesion for composites containing natural fibres and fillers is generally achieved by means of one of the following ways: fibre modification, the use of interface-active additives or matrix modification. Fibre modification involves grafting functional groups on the lignocellulosic fibres or coating fibres with additives that carry suitable functional groups, in order to make the fibre surface more compatible/reactive to the matrix material. The various reactive species that can be used for fibre modification include one or more of the following: acetic anhydride, *n*-alkyl isocyanates, styrene, maleic anhydride and silanes. The second method for promoting interfacial adhesion involves the use of additives that act as coupling agents. Polyesteramide polyol, titanates, chemicals based on trichloro-s-triazine, poly[methylene (polyphenylisocyanate)], maleic anhydride and silanes can been employed for this purpose. The use of interface-active additives is the least effective method for improving adhesion characteristics, while matrix modification is a quick and effective method. In contrast, fibre modification, which is also an effective method, mostly involves solvent-based processes, which are slower and not very attractive environmentally nor also from a commercial point of view [22]. This method is also strongly influenced by changes in aspect ratio. As the compounding progresses, the initial area of the fibres increase due the decrease in both diameter and length, so the final interface area increases with respect to the initial one.

Fibre aspect ratio is the parameter that suffers added modifications during compounding. Although cellulose fibres are flexible, the interaction between fibre

and fibre, fibres and matrix and between processing equipment is also strongly dependent on the concentration; in particular, the interaction increases with an increase in concentration. However, it is important to note that the interaction also depends on fibre flexibility. For rigid glass fibre reinforced polypropylene compounded in a single screw extruder, the fibre damage increases with an increase in fibre concentration [23, 24]. However, in the case of flexible flax cellulose fibre reinforced polypropylene compounded in a mixer, the damage decreases as fibre concentration increases, due to the ability of the fibre to entangle.

In this study, fibre structure variation during the processing of polypropylene matrix reinforced with cellulose flax pulp for different reinforcement concentrations (0, 10, 20, 30 and 40 wt%) is analyzed. The effect of the microstructure variation on the final mechanical properties is studied and a systematic study of the aspect ratio variation with compounding and concentration and its influence on final properties is proposed.

In particular, the interfacial area was evaluated, considering fibres to be cylinders with average values of diameters and lengths calculated using a statistical distribution approach. The volume and the surface of the single fibre in the different compositions and for the pure fibres before the processing were calculated using previous parameters and the value of the interfacial area in the unit volume for each composite was calculated.

2. EXPERIMENTAL

Polypropylene powder MOPLEN FL F20 (M_w: 240000 g/mol; M_n: 94000 g/mol) kindly supplied by Montell, was used as a matrix; this selection was adopted for the better mixing properties of powder in comparison with standard PP pellets. Natural fibres from cellulose pulp sheets were used as reinforcements. The cellulose pulp type LINCELL A, was kindly supplied by Celesa. The dispersion of the cellulose fibre in the polypropylene was very difficult since the adhesion between fibres in the sheets was very high. For this reason, the sheets were ground in a high speed rotational mill at room temperature for 2 min at 1000 rpm. After this process, the fibres were separated properly and the final pulp was very similar to cotton wool.

The cellulose composites were obtained by melt compounding in a counter rotating twin screw extruder BAUSANO MD 30 model at 20 rpm; the fibres were introduced in two subsequent steps, in order to add all the fibre amount in the matrix, thereby obtaining a better dispersion. Samples with concentrations of 10, 20, 30 and 40 wt% were prepared. In Table 1, the corresponding volume fractions are reported. The fibre density was measured according to the ASTM D 792 regulations and a value of 1.35 ± 0.04 g/cm^3 was obtained.

The previous mixing procedure was selected after several tests in different conditions but only the grinding of cellulose pulp guaranteed the necessary dispersion level of the fibres. Fibre dispersion in the matrix and the characterization of the

Table 1.
Name and concentration of all composites prepared

Denomination	Fibre weight fraction (ϕ)	Fibre volume fraction (ϕ_v)
C0 (PP)	0	0
C10	0.10	0.069
C20	0.20	0.143
C30	0.30	0.222
C40	0.40	0.308

structure in terms of geometrical parameters was obtained by means of transmission light optical microscopy, with a model H600 Hund Wetzlar microscope. The image analysis was performed using 4.0 Scion image software. There were different acquisitions at different magnification levels in order to analyze all the geometrical parameters of the fibres better. In particular, the length was analyzed using a 2.5× magnification and the diameter was measured with images at 10× magnification. Due to fibre flexibility, the analysis of the geometrical parameter was difficult; in fact, the diameter was not constant for all the fibre lengths. Moreover, the fibres had to be fitted with a sequence of straight segments in order to measure the length.

The geometrical parameters of the fibre were measured before and after fibre grinding and after compounding for each fibre concentration. In the case of pure fibres, the measurements were taken by dispersing the cellulose in water and putting the fibres onto the glass slides directly for microscopic observations. In the case of the composites, the measurements were taken by melting and compressing a small part of the material between two glass slides. By using this method, a transparent thin film was obtained and measurements under the microscope could be taken. At least 30 images and 150 measurements were taken for each sample in order to obtain the statistical distribution of the lengths, diameters and aspect ratios of the fibres.

A mechanical characterization of the fibres and composites (tensile test) was performed with a model LR 30K Lloyd electronic dynamometer. The fibres used to produce the cellulose pulp were tested in accordance with the ASTM D 3379 regulations and the results were analyzed on the basis of a Weibull distribution. Samples with different gauge lengths (10, 20, 30 and 40 mm) were tested at a strain rate of 1 mm/min, using a load cell of 5 N and at least 10 samples for each gauge length were tested. The polypropylene matrix and the composites were tested according to the ASTM D638 regulations at a load cell of 30 kN and at a strain rate of 5 mm/min and at least 5 samples for each material was tested.

A SUPRA 25 FESEM Zeiss was used for the analysis of fracture surfaces of samples after tensile tests.

3. RESULTS AND DISCUSSION

The experimental studies performed before compounding showed that the fibre dimensions suffered only few changes after the grinding of the cellulose pulp (this

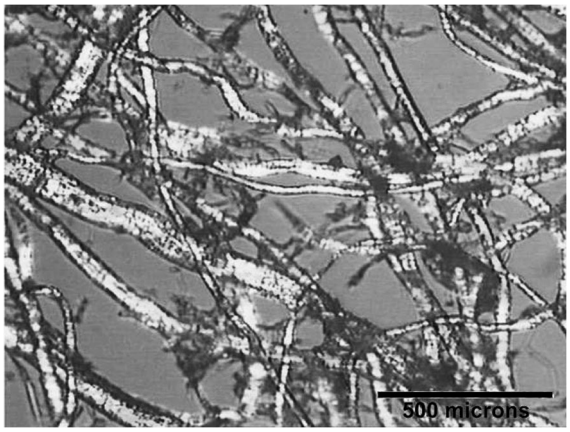

(a)

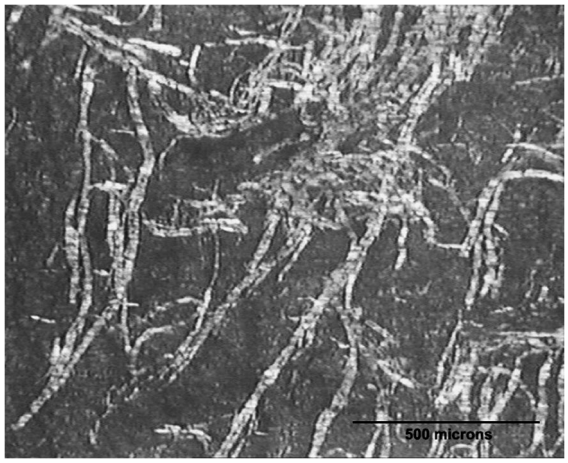

(b)

Figure 1. Optical micrograph of cellulose fibre before compounding and after grinding (a) and in the C30 composite (b).

step is essential for good dispersion). Previous experimental results demonstrated that average length changed approximately 4% from the initial values [25], but the average diameter variation is one order of magnitude less. The aspect ratio, as expected, decreased to 4% since the variation in length was greater than the one in diameter. Optical microscope images of fibres after grinding and before processing are shown in Fig. 1(a) and Fig. 1(b), in which the flexibility of the fibres and their non-constant diameter and length is observed.

The difference in the fibre's geometrical parameters is more noticeable after compounding. Table 1 shows the mean values obtained after microscopic measurements and Fig. 2 shows the aspect ratio distribution (normalized area) for all of the prepared composites, using the statistical approach described in the Appendix. The average length decreased 8.5 times for composites with 10 wt% in fibres, 7 times

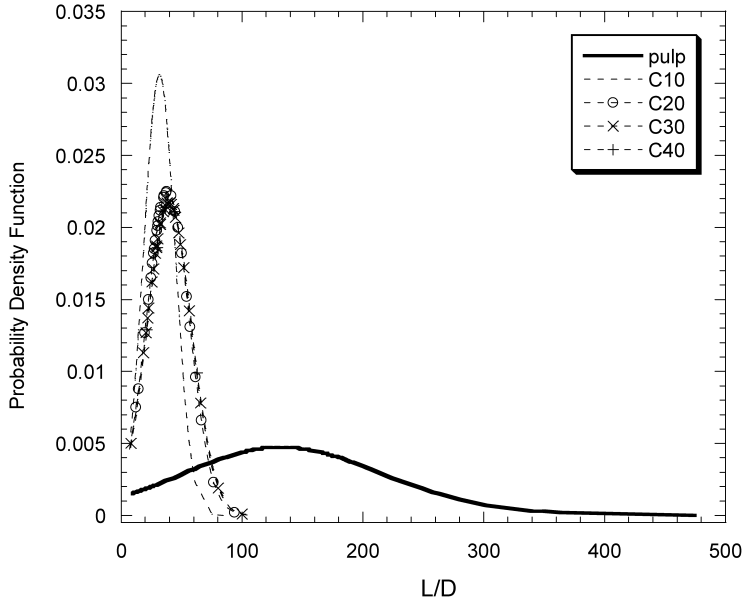

Figure 2. Fibre aspect ratio distribution after compounding for all prepared composites.

for those with 20 wt% and around 6.5 times for higher concentrations: the lower the fibre concentration, the narrower the fibre length distribution. It seems that, when considering critical concentrations, the fibres suffered the same kind of damage and therefore the length distributions for 30 wt% and 40 wt% match each other.

The fibre diameter distributions show similar behaviour to that of fibre lengths. Compositions with 10 wt% in fibres suffered a decrease of 58% in the average diameter, while for the 20 wt% composition, the diameter was reduced to 70% of the initial value, and for the other two compositions (30 and 40 wt%), there was an 86% decrease.

The aspect ratio (L/D) also increased with an increase in fibre concentration. This means that as the concentration increases, the decrease in diameter is more pronounced than the length (Fig. 3(a) and 3(b)).

This has been analyzed and justified in a previous study [25], taking into account the increment in fibre entanglement, due to higher concentration impeding fibre movement and consequent length attrition.

In order to analyze area variation after compounding for each concentration, fibres in the form of flexible cylinders, having the dimensions equal to the average values of diameters and lengths, were considered and calculated with a statistical distribution. This estimate was based on previous microscopical studies of fibres. They are almost circular strands of fibrils [26]. The volume and the surface area of the single fibre, both in its pure form and as a composite, were calculated, taking the modification induced by the processing into account. It was possible to calculate the number of fibres in the unit volume of each composition by applying

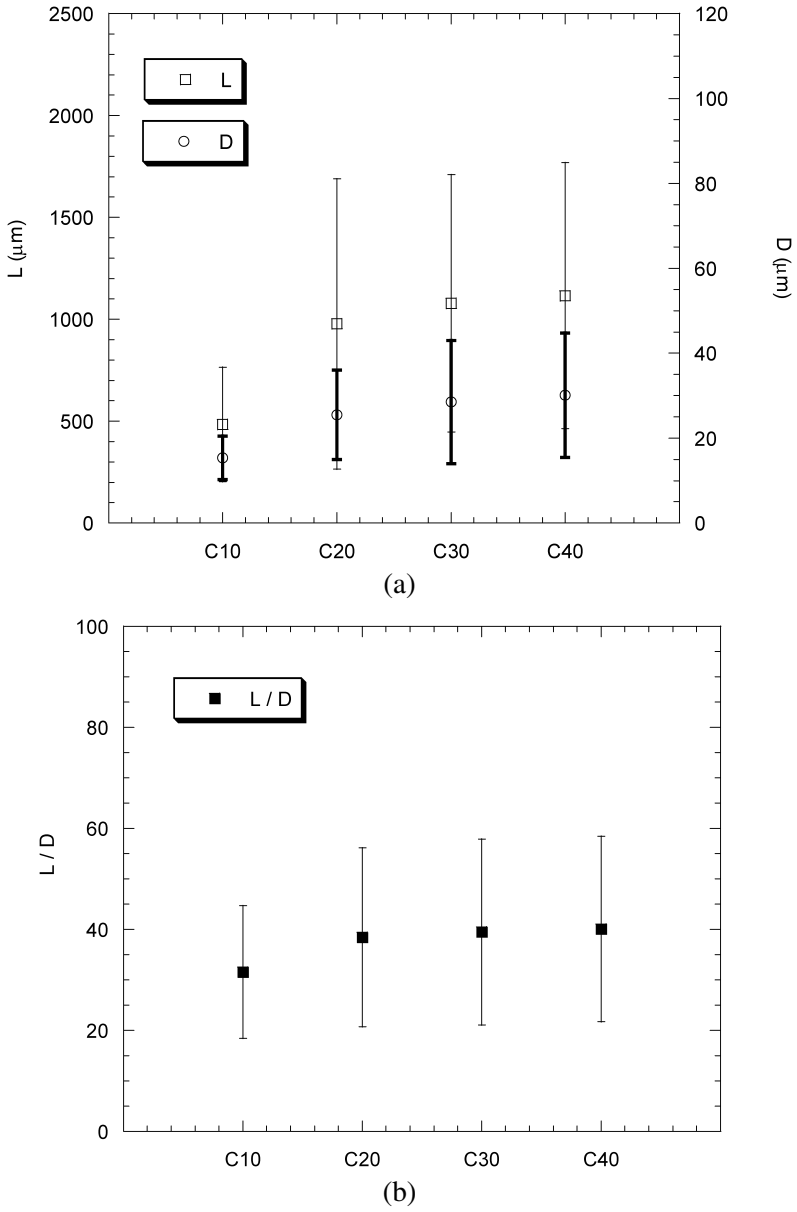

Figure 3. Average values of the geometrical parameters of cellulose fibres after compounding. (a) Geometrical dimensions L and D; (b) ratio L/D.

the volume of the single fibre and the volume fraction of the reinforcements in the composites. When the number of fibres was obtained, it was possible to calculate the interfacial area in the unit volume of each composite. The data related to this calculation are reported in Figs 4(a) and 4(b). From these data, it is clear that the superficial fibre area decreases forty times when compounding is performed on

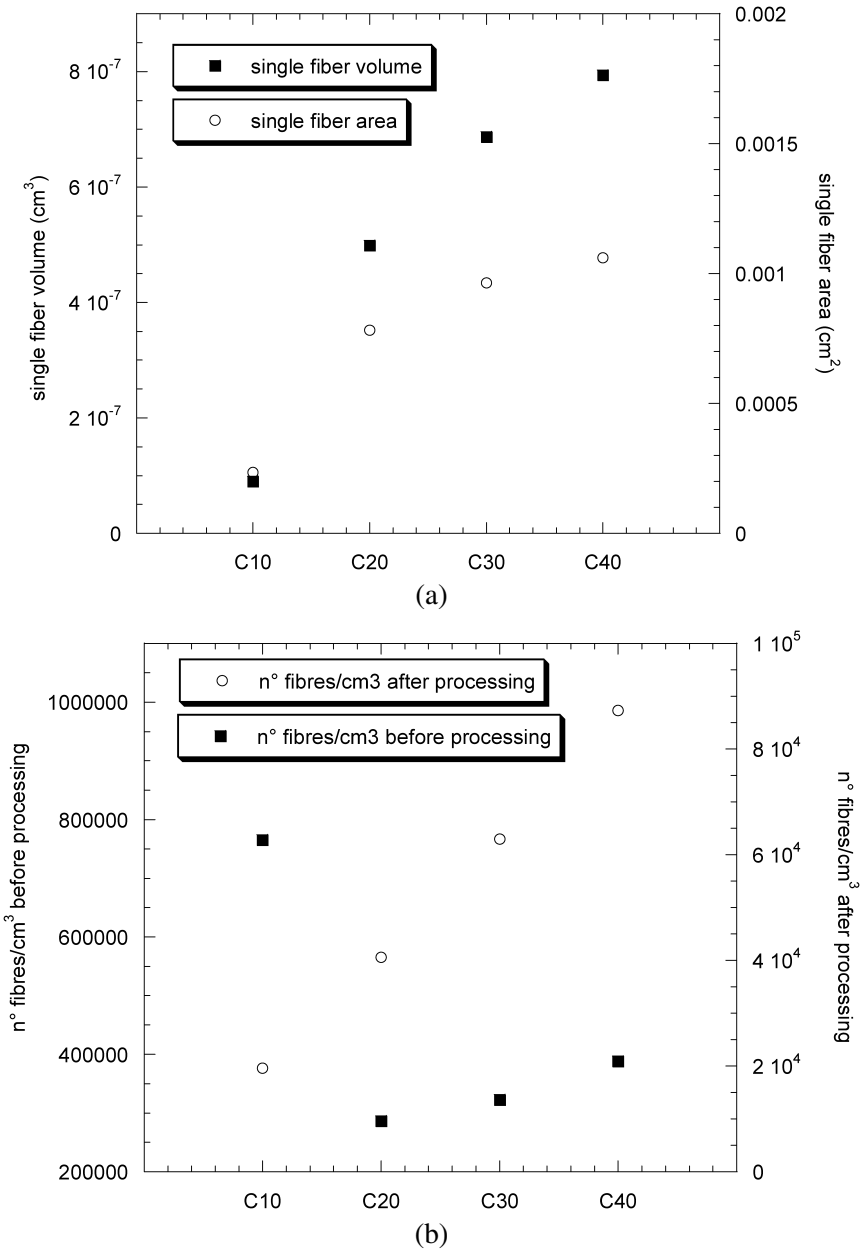

Figure 4. Fibre volume and surface (a), and number of fibres for unit volumes of composites before and after processing (b).

small fibre concentration composites (10%). However, the interfacial area decreases four times when the fibre concentration is 40%. The influence of the concentration on the interfacial area is therefore evident. In Fig. 5, the fibre surface for a unit volume composite is reported. It can be seen that, during the processing operation,

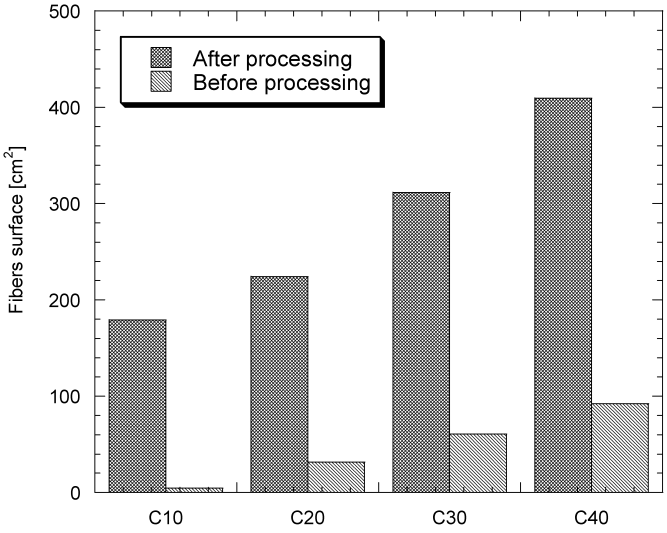

Figure 5. Fibre surface in any unit volume composite before and after the processing operation.

the fibre surface increases significantly. In fact, the initial fibre bundle is separated until it nearly reaches the single fibre unit (15 μm diameter) in the composites, in the case of 10 wt% reinforcement. For the other composites, taking the dimensions obtained for the diameter into account, it could be estimated that after processing, only bundles with few fibres remain in the material.

Literature reports several studies regarding the effect of compatibilization treatments for natural fibre, where the compatibizer is directly combined on the fibre surface before compounding. However, as demonstrated, taking into account the measurements performed on fibre diameters, the initial fibre bundles were separated during processing; consequently, a large fraction of untreated surface should be in contact with the matrix, making this compatibilization treatment less effective. Moreover, the effectiveness depends on fibre concentration (if we consider the changes in the exposed area only). On the basis of this consideration, in our opinion, it is possible to assert that the compatibilization of the matrix (such as maleic anhydride) is more effective than the treatment of the fibres. In fact, when compatibilizer is used in the matrix, the agent is present in the entire interface volume between fibres and matrix, and there is no limitation due to the lack of compatibilizer in some regions of the fibre surface.

After the elaboration of these parameters, the flax cellulose fibres used to produce the pulp were mechanically tested. The Weibull cumulative density function for the strength $F(\sigma)$ was considered and the same approach was used for the analysis of the E modulus (equation (1)):

$$F(E) = \exp\left\{-\left(\frac{E}{E_0}\right)^q\right\}, \tag{1}$$

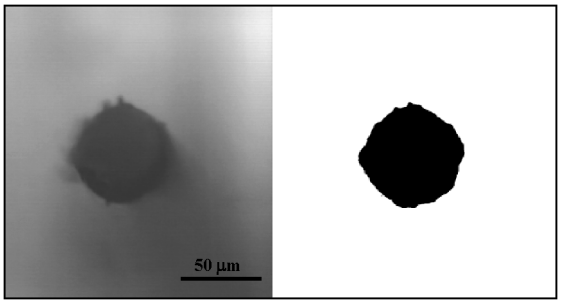

Figure 6. Evaluation by imaging software elaboration of cross-sectional area for the flax cellulose fibre.

$$P(E) = |D[F(E)]|, \tag{2}$$

where $F(E)$ is the survival probability of the fibre with modulus E, q is a dimensionless shape factor and E_0 is the scale parameter. In equation (2), $D[F(E)]$ is the derivate of the probability that the fibres have the modulus E and $P(E)$ is the cumulative probability.

The calculation of the mechanical parameters requires knowledge of the cross-sectional area of the fibres. The cross-sectional area of each fibre (Fig. 6) was analysed using an optical microscope and 4.0 Scion Image software was used to determine the numerical value. This procedure was required due to the irregular shape of the cross-section.

The function $F(\sigma)$ is set out in a log–log diagram in Fig. 7(a) and a comparison between the experimental data and model is reported in Fig. 7(b).

The same procedure was used for the analysis of the failure strain and for the determination of the $F(E)$ in the Young's modulus analysis. Using equation (2), the diagram in Fig. 8 could be plotted and the statistical value of Young's modulus was determined. In particular, the average modulus corresponds to the point where the cumulative probability is at a maximum and the standard deviation can be calculated taking the values of the modulus corresponding to the half height of the curve maximum into consideration [27].

The final values of typical parameters for fibres [28] and PP matrix are reported in Table 2. Thereafter, it was possible to determine the mechanical parameters of PP flax fibre composites from tensile tests (Figs 9 and 10).

In order to verify the experimental data obtained from the tensile tests for the different composites and considering different fibre aspect ratios and interfacial area values obtained for the composite blends, the Halpin–Tsai model [29] was applied. Concerning the application of the Halpin–Tsai equations to the natural fiber composite, a more accurate modelling of the composite mechanical properties can be obtained by using the measured values of the geometrical dimensions and the predicted values of the respective moduli. Such an operation can be completed with the help of statistical distribution of the properties of the composites, which, by taking into account the above expressed property variations, is able to embody the

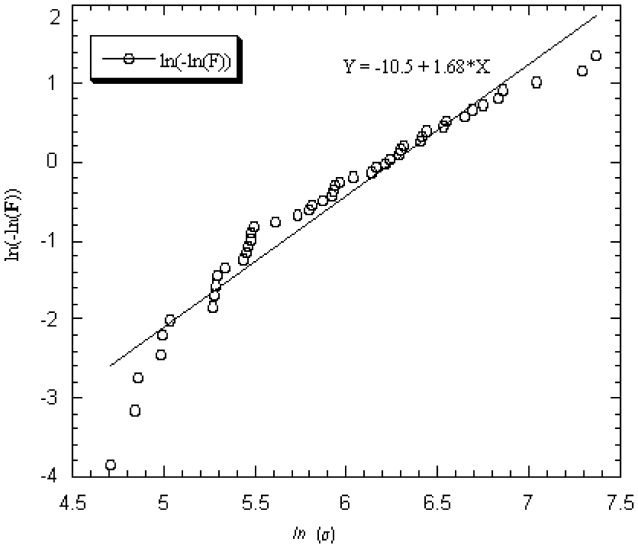

(a)

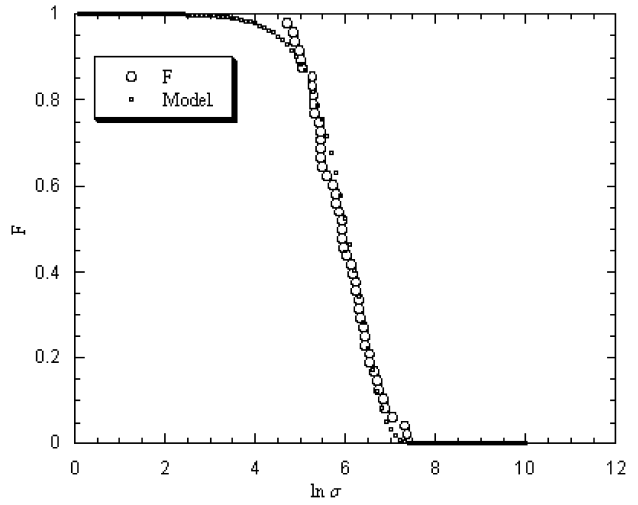

(b)

Figure 7. (a) Diagram of the $\ln(-\ln F(\sigma))$ as a function of $\ln(\sigma)$; (b) Comparison between experimental data and Weibull model for $F(E)$.

rich information content of the measured data. In this work, the values of the moduli of the composites are not directly calculated using a single geometrical parameter in the Halpin–Tsai equations, but the modal values of statistical distribution are considered, which allow one to take into account the different possible combinations of fiber aspect ratios and interfacial area variation.

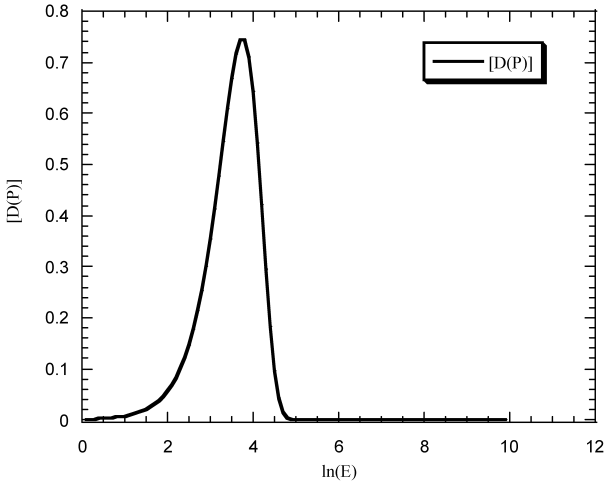

Figure 8. Theoretical model of the statistical probability of the Young modulus.

Table 2.
Mechanical parameters of the flax fibre used to produce the cellulose pulp (obtained by Weibull distribution calculation) and PP matrix

	Flax fibres	PP matrix
Young's modulus (GPa)	27.0 ± 2.1	1.150 ± 0.025
Tensile strength (MPa)	523 ± 1.7	33.5 ± 1.5
Failure strain (%)	0.0022 ± 0.001	>200

According to this model, the elastic modulus of the composite is expressed by the following equations:

$$E = \frac{3}{8}E_{11} + \frac{5}{8}E_{22}, \tag{3}$$

where:

$$E_{11} = \frac{1 + 2(l_f/l_d)\eta_L V_f}{1 - \eta_L V_f}E_m, \tag{4}$$

$$E_{22} = \frac{1 + 2\eta_T V_f}{1 - \eta_T V_f}E_m, \tag{5}$$

$$\eta_L = \frac{(E_f/E_m) - 1}{(E_f/E_m) + 2(l_f/d_f)}, \tag{6}$$

$$\eta_T = \frac{(E_f/E_m) - 1}{(E_f/E_m) + 2} \tag{7}$$

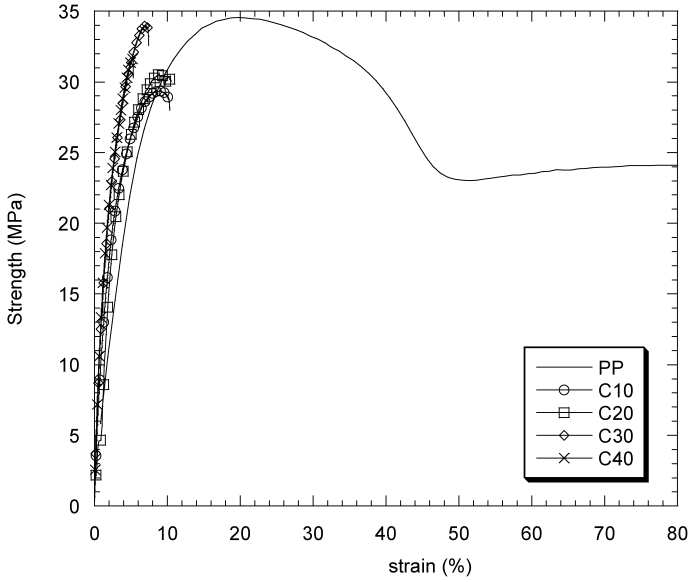

Figure 9. Stress–strain curves for neat PP and flax cellulose composites.

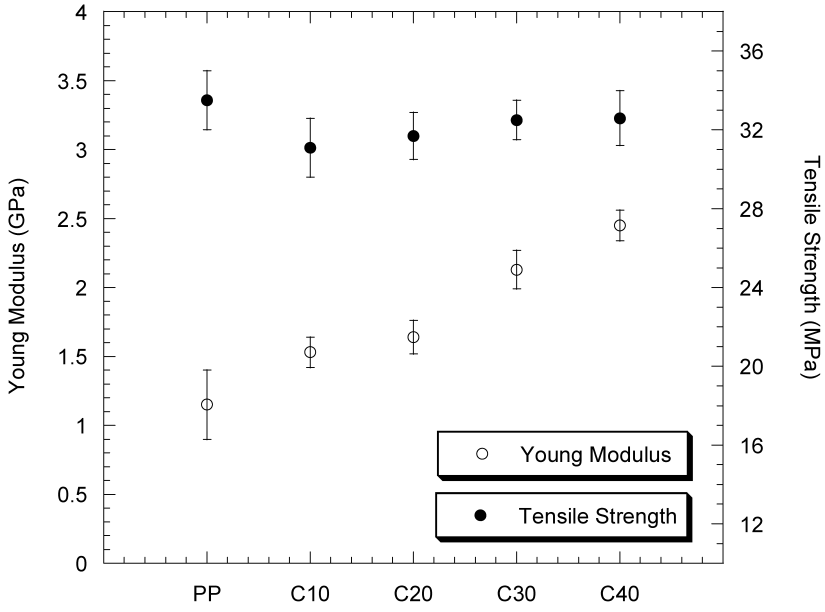

Figure 10. Mechanical parameters of the PP and cellulose composites.

and: E_m is the elastic modulus of the matrix in the absence of fibre, E_f is the elastic modulus of the flax fibre, V_f is the percentage in volume of the flax fibre, d_f is the average diameter of the flax fibre and l_f is the average length of the flax fibre.

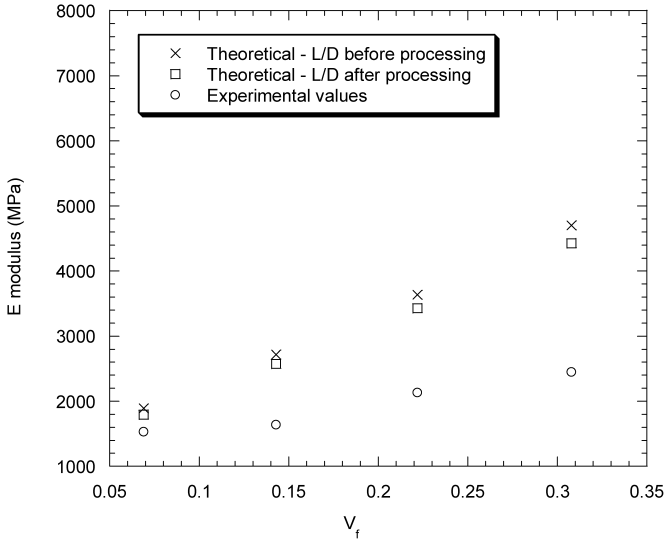

Figure 11. Comparison between experimental and model values for elastic modulus of PP cellulose composites.

The values of the elastic modulus for cellulose/PP composites *versus* fibre volume fraction are reported in Fig. 11, where the Halpin–Tsai predictions for the fibre composite moduli are reported; the values for L/D fibre aspect ratio before and after the processing step are reported, in order to verify the effect of interfacial area variation in the final tensile properties of the composites (the calculations were performed considering final L/D values in the composites (after processing) and initial values after grinding but before compounding (before processing). However, it is possible to notice that, in all cases, the theoretical modal values of the mechanical properties described are slightly greater in comparison to the measured experimental values: the deviation of the real composite features from the basic assumptions of the theoretical approach, where a perfect adhesion at the fiber/matrix interface and an absence of voids are required [30], can also contribute to the disagreement between experimental data and the model. The confirmation of a weak interface between fibre and matrix is given by the analysis of the fracture surface micrographs (Fig. 12). In these images, it is possible to observe that, during tensile failure, fibre pull-out occurs, due to poor compatibility between fibre and matrix. These results were as expected, since compatibilization treatment was not considered both for fibres and matrix.

4. CONCLUSIONS

The studies performed in the present paper allow the analysis of the influence of aspect ratio modifications during compounding and its influence on either the

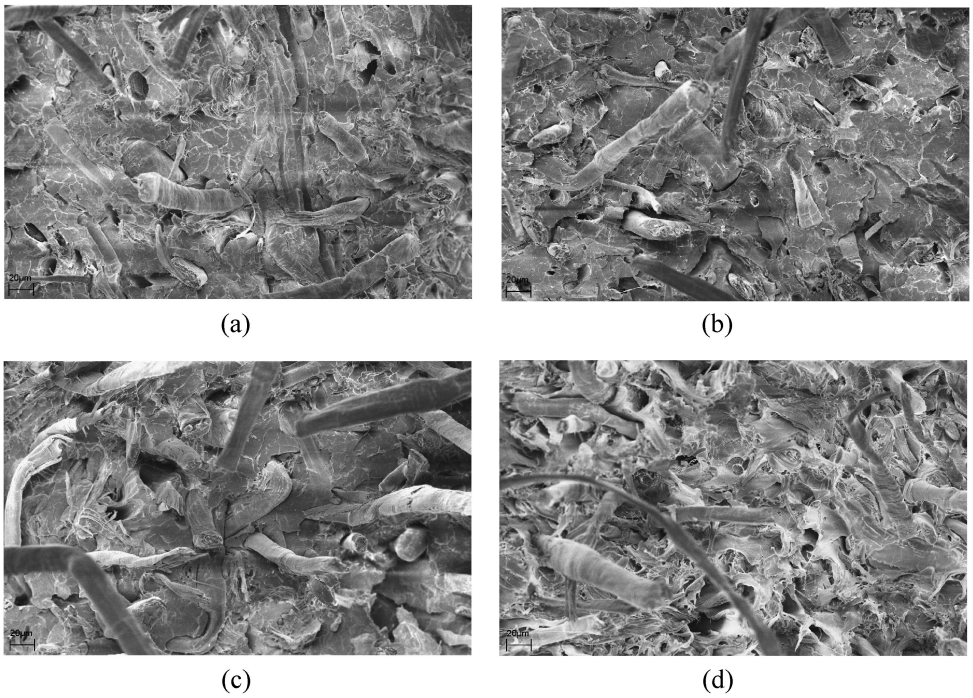

Figure 12. SEM micrographs of (a) C10, (b) C20, (c) C30 and (d) C40 composites.

adhesion improvement methods or on the final properties. In this regard, the main conclusions obtained are:

– Although they are flexible, fibres break under compounding for both fibre–fibre interaction and for fibre-equipment wall attrition.
– The attrition involves both the diameter (bundle separation) and length and leads to changes in the aspect ratio and interfacial area.
– The attrition decreases as the concentration increases because of fibre entanglements.
– The interfacial area is strongly dependent on fibre concentration: the lower the concentration, the higher the interfacial area.
– The adhesion process usually involves fibre surface modification in order to improve adhesion. However, the higher the concentration, the more the surface increases and the less effective is the modifier in the same order. Therefore, it is more important to compatibilize the matrix rather than the fibre itself in order to obtain better final properties for the fibre reinforced composite.
– The theoretical approach used for the estimation of elastic moduli should consider the effect of L/D parameter and variation in interfacial area for fibres at different concentrations. This kind of modelling allows a better characterization of natural fiber composites which mechanical properties are strongly affected by the broad distribution of fiber dimensions.

REFERENCES

1. P. Wambua, J. Ivens and I. Varpoest, Natural fibres: can they replace glass in fibre reinforced plastics? *Compos. Sci. Tech.* **63**, 1259–1264 (2003).
2. I. Van de Weyenberg, T. Chi Truong, B. Vangrimde and I. Verpoest, Improving the properties of UD flax fibre reinforced composites by applying an alkaline fibre treatment, *Composites: Part A* **37**, 1368–1376 (2006).
3. T. Hartness, G. Husman, J. Koenig and J. Dyksterhouse, The characterization of low cost fibre reinforced thermoplastic composites produced by the DRIFT^{TM} process, *Composites: Part A*, **32**, 1155–1160 (2001).
4. P. V. Joseph, K. Joseph and S. Thomas, Effect of processing variables on the mechanical properties of sisal-fibre-reinforced polypropylene composites, *Compos. Sci. Technol.* **59**, 1625–1640 (1999).
5. M. Baiardo, E. Zini and M. Standola, Flax fibre–polyester composites, *Composites: Part A* **35**, 703–710 (2004).
6. Y. Li, Y. W. Mai and L. Ye, Sisal fibre and its composites: a review of recent developments, *Compos. Sci. Technol.* **60**, 2037–2055 (2000).
7. R. M. Rowell, A. R. Sanadi, D. F. Caulfield and R. E. Jacobsen, Utilization of natural fibres in plastic composites: problems and opportunities, in: *Lignocellulosic-Plastic Composites*, A. L. Leão, F. X. Carvalho and E. Frollini (Eds), pp. 23–51. São Paulo, USP and UNESP (1997).
8. G. Canchè-Escamilla, J. Rodriguez-Lavida, J. I. Cauich-Cupul, E. Mendizàbal, J. E. Puig and P. J. Herrera-Franco, Flexural, impact and compressive properties of a rigid-thermoplastic matrix/cellulose fibre reinforced composites, *Composites: Part A* **33**, 539–549 (2002).
9. J. George, R. Janardhan, J. S. Anand, S. S. Bhagawan and S. Thomas, Melt rheological behavior of short pineapple fibre reinforced low density polyethylene composites, *Polymers* **37**, 5421–5431 (1996).
10. A. Stamboulis, C. A. Baille and T. Peijs, Effects of environmental conditions on mechanical and physical properties of flax fibres, *Composites: Part A* **32**, 1105–1115 (2001).
11. M. M. Thwe and K. Liao, Effects of environmental aging on the mechanical properties of bamboo-glass fibre reinforced polymer matrix hybrid composites, *Composites: Part A* **33**, 43–52 (2002).
12. H. Larbig, H. Scherzer, B. Dahlke and R. Poltrock, Natural fibre reinforced foams based on renewable resources for automotive interior applications, *J. Cell. Plast.* **34**, 361–379 (1998).
13. A. Leao, R. Rowell and N. Tavares, Applications of natural fibres in automotive industry in Brazil-thermoforming process, in: *Proc. 4th Internat. Conf. Frontiers Polym. Adv. Mater.*, Cairo, Egypt, Plenum Press, pp. 755–760 (1997).
14. G. Marsh, Next step for automotive materials, *Materials Today* **4**, 27–33 (2003).
15. R. A. Young, Utilization of natural fibres: characterization, modification and applications, in: *Lignocellulosic-Plastics Composites*, A. L. Leao, F. X. Carvalho and E. Frollini (Eds). USP and UNESP, Brazil (1997).
16. R. A. Young, A. Sanadi and S. Prabawa, Effect of extractives and fibre surface properties on sisal fibre propylene composites, in: *Proc. 4th Internat. Conf. Wood Fibre-Plastic Compos.*, Forest Products Society, Madison, USA, pp. 5 (1997).
17. P. Gatenholm, H. Bertilsson and A. Mathisson, The effect of chemical composition of interphase on dispersion of cellulose fibres in polymers. I. PVC-coated cellulose in polystyrene, *J. Appl. Polym. Sci.* **49**, 197–208 (1993).
18. M. M. Sain and B. V. Kokta, Polyolefin-wood filler composite. I. Performance of m-phenylene bismaleimide-modified wood fibre in polypropylene composite, *J. Appl. Polym. Sci.* **54**, 1545–1559 (1994).
19. M. Sain, P. Suhara, S. Law and A. Bouilloux, Interface modification and mechanical properties of natural fibre-polyolefin composite products, *J. Reinf. Plast. Compos.* **24**, 121–130 (2005).

20. H. Cabral, M. Cisneros, J. M. Kenny, A. Vazquez and C. R. Bernal, Structure-properties relationship of short jute fibre-reinforced polypropylene composites, *J. Compos. Mater.* **39**, 51–65 (2005).
21. M. G. El-Meligy, W. K. El-Zawawy and M. M. Ibrahim, Lignocellulosic composite, *Polym. Adv. Technol.* **15**, 738–745 (2004).
22. D. Puglia, J. Biagiotti and J. M. Kenny, Review on natural fibre-based composites — Part II: Application of natural reinforcements in composite materials for automotive industry, *J. Natural Fibres* **1**, 23–65 (2005).
23. G. B. Nando and B. R. Gupta, Short fibre-thermoplastic elastomer composites, in: *Short Fibre-Polymer Composites*, J. R. White and S. K. De (Eds). Woodhead Publishing, Cambridge, UK (1996).
24. S. E. Barbosa and J. M. Kenny, Processing of short-fibre reinforced polypropylene. I. Influence of processing condition on the morphology of extruded filaments, *Polym. Engng. Sci.* **40**, 11–22 (2000).
25. A. Terenzi, J. M. Kenny and S. E. Barbosa, Natural fibre composites in thermoplastic polymers: I. Analysis of fibre damage during processing, *J. Appl. Polym. Sci.* **103**, 2501–2506 (2007).
26. J. Biagiotti, D. Puglia and J. M. Kenny, A review on natural fibre based composites Part 1: Structure, processing, and properties of vegetable fibres, *J. Natural Fibres* **1**, 37–68 (2005).
27. M. Baiardo, E. Zini and M. Standola, Flax fibre–polyester composites, *Composites: Part A* **35**, 703–710 (2004).
28. K. Gamsted, *Estimation of strength properties of single carbon fibres from boundle testing*, Msc Thesis, Division of Polymer Engeneering, Lulea University of Technology, Sweden, (1996).
29. C. Halpin and J. L. Kardos, The Halpin–Tsai equations: a review, *J. Polym. Engng. Sci.* **16**, 344–352 (1976).
30. G. S. Holister and C. Thomas, *Fiber Reinforced Materials*. Elsevier Publishing Co., London, UK (1966).

APPENDIX

The distributions of the geometrical parameters were assessed using the calculation of the probability density of the acquired data. EM algorithm and 5.3 MATLAB software were used for the previous calculations. This algorithm works with a linear combination of Gaussian functions and, in this study, the class described by the following equations were used:

$$p(x|\theta) = \sum_{i=1}^{n} \kappa_i N(x|\mu_i \Sigma_i), \tag{A.1}$$

where θ is a vector with components $(\kappa_i,\ \mu_i,\ \Sigma_i)_{i=1}^{n}$ subject to the following constraints: $\kappa_i \geqslant 0$ and $\sum_{i=1}^{n} \kappa_i = 1$. The term $N(x|\mu_i \Sigma_i)$ is the normal density (or Gaussian one) give by equation (A.2).

$$N(x|\mu_i \Sigma_i) = (2\pi)^{-d/2} |\Sigma_i|^{-1/2} \exp\left[-\frac{1}{2} \cdot \frac{(x-\mu_i)^i}{\Sigma(x-\mu_i)} \right]. \tag{A.2}$$

The parameters in equations (A.1) and (A.2) can be calculated iteratively using a EM algorithm. The iterations are divided into two steps. The first one (step E) allows the estimation of the current parameters:

$$h_i^k = \frac{\kappa_i V(x^k|\mu_i \Sigma_i)}{\sum_{j=1}^{n} \kappa_j N(x|\mu_i \Sigma_i)}. \tag{A.3}$$

The second step, called M, permits one to obtain the new parameters by means of:

$$\kappa_i = \frac{1}{m} \sum_{k=1}^{m} h_i^k, \tag{A.4}$$

$$\mu_i' = \frac{\sum_{k=1}^{m} h_i^k x^k}{\sum_{l=1}^{m} h_i^l}, \tag{A.5}$$

$$\Sigma_i' = \frac{\sum_{k=1}^{m} h_i^k (x^k - \mu_i')(x^k - \mu_i')^{\mathrm{T}}}{\sum_{l=1}^{m} h_i^l}. \tag{A.6}$$

The probability density of the geometrical parameters measured was calculated by an iteration of this algorithm up to convergence. It is important to note that it is not possible to obtain the analytical expression of the distribution with this algorithm.